Decorating Polar Zonohedra with Islamic Geometric Patterns

Phil Webster

Phil Webster Design, Chandler, AZ, USA; phil@philwebsterdesign.com

Abstract

This paper describes a process for applying Islamic geometric patterns (IGP) to the faces of polar zonohedra (PZ). First, a process for developing IGP that repeat on rhombic grids is presented. Then, PZ are defined and the formula for calculating the rhombic face angles is shown. Since the set of face angles for a given PZ is almost never identical to those of the rhombic grids for IGP, a system is presented for systematically identifying PZ and IGP whose rhombic angles are within a given threshold. IGP can then be applied to the faces of the identified PZ using small linear scaling factors — making distortions practically unnoticeable to the naked eye.

Background and Motivation

Having spent many years decorating polyhedra (primarily Platonic and Archimedean solids) with Islamic geometric patterns (IGP), I became interested in whether they could also be applied to polar zonohedra (PZ). As Figures 1 and 9 show, I discovered that it is, in fact, possible. However, PZ must be chosen according to a fairly strict set of criteria in order for the final pattern to appear undistorted and aesthetically pleasing.

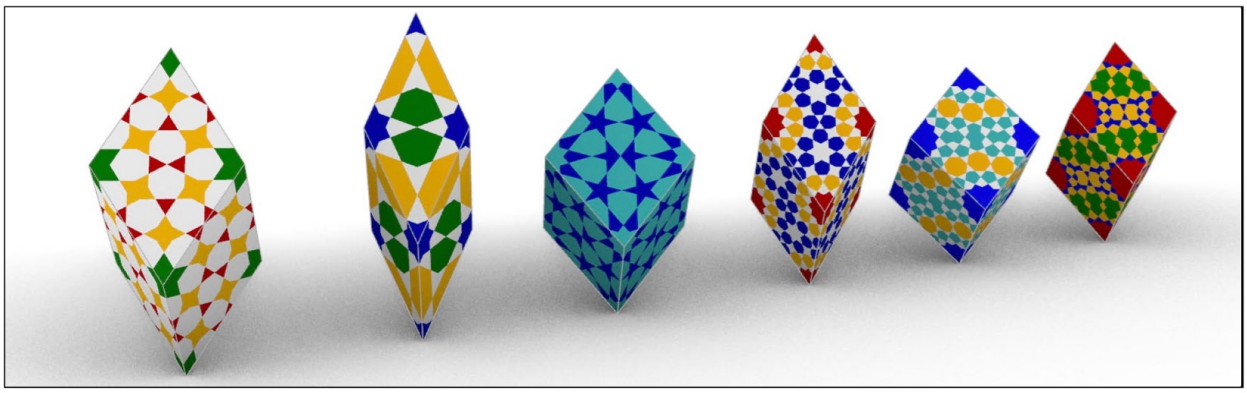

Figure 1: *A series of $PZ(3,\theta)$ fitting various $IGP_R(N)$, with $N \in \{6,8,10,12,14,16\}$ (left to right).*

Introduction to Islamic Geometric Patterns

The field of IGP is a vast one, and many Bridges papers by myself [7] and other authors [2, 3, 6] have explored ways of extending this tradition in new directions beyond the designs found in the historical record. Traditional IGP generally repeat in the plane, as an expression of the infinite. All of the familiar planar repeat units such as squares, rectangles, triangles, and hexagons appear regularly. Another common repeat unit is the rhombus, and many successful traditional patterns follow this repeat scheme as well [1]. In particular, there is a systematic way to develop IGP whose primary motifs have N-fold symmetry, and whose repeat units are rhombi with angles of the form $i(360/N)^\circ$ where i is a positive integer.

Creating N-fold IGP with Rhombic Repeat Units

Consider a rhombus whose angles are $a(360/N)^\circ$ and $b(360/N)^\circ$ for positive integers a, b, and N, with $a \leq b$. Since the angles sum to 180°, we have $a(360/N) + b(360/N) = 180$, so $(2a + 2b) = N$. Thus N must be even, and $a + b = N/2$. Setting $a = b = 1$ yields $N = 4$, i.e. a square, which is not of interest for this investigation. Also, developing reasonable IGP, especially on the thinnest rhombi ($a = 1$) becomes increasingly challenging as N increases. Thus, I will be considering rhombic repeat units where N is even and $6 \leq N \leq 16$. For each such N there are $\lfloor N/4 \rfloor$ distinct pairs (a, b). ***Henceforth a set of edge-matched IGP for all rhombic repeat units for a given N will be called*** $\mathbf{IGP_R(N)}$**.** Figure 2 shows examples of $IGP_R(N)$ for $6 \leq N \leq 16$.

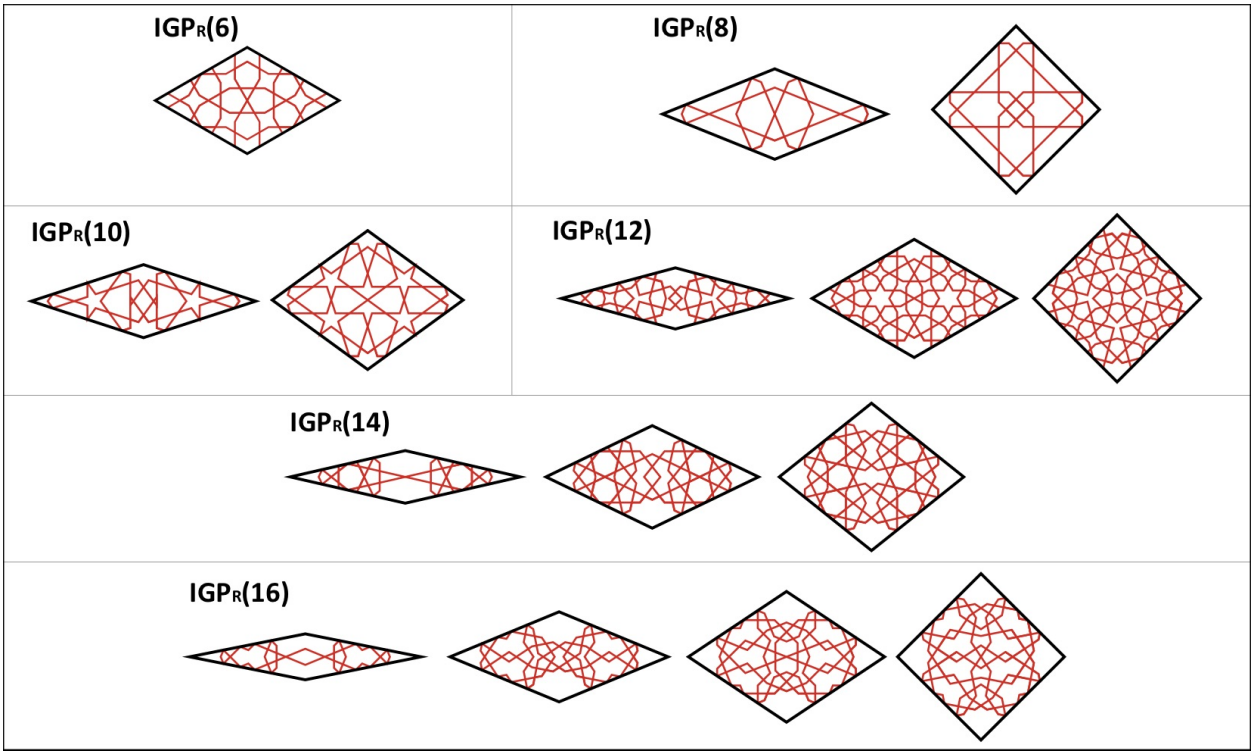

Figure 2: *Examples of $IGP_R(N)$ for $N \in \{6, 8, 10, 12, 14, 16\}$.*

Figure 3 illustrates the steps for developing $IGP_R(N)$, using $N = 10$ as an example. First, we create all possible rhombi with acute angles $a(360/N), 1 \leq a \leq \lfloor N/4 \rfloor$ and place centers of N-fold symmetry at the vertices. Then, using well documented techniques [1, 5] we develop a polygonal subgrid for each rhombus. Note that for small a, it is common practice to allow the N-fold polygons at the obtuse vertices to overlap and merge in the center of the rhombus. One important additional constraint is that we must find subgrids for all rhombi in the family that have the same configuration along every edge (hence "edge-matched" in the definition above). This will assure that rhombi of different shapes can still match edge to edge across the entire range of faces in a given PZ. Once all subgrids have been created, we place pairs of lines at each midpoint, crossing at a consistent contact angle, and extend those lines to complete the pattern. As with all IGP, there are often multiple possible subgrids, as well as multiple families of patterns on a given subgrid depending on the choice of contact angle (acute, median, obtuse, and/or two-point, per Bonner's terminology [1]) that can be developed on a given subgrid; only one example pattern for each N is shown here.

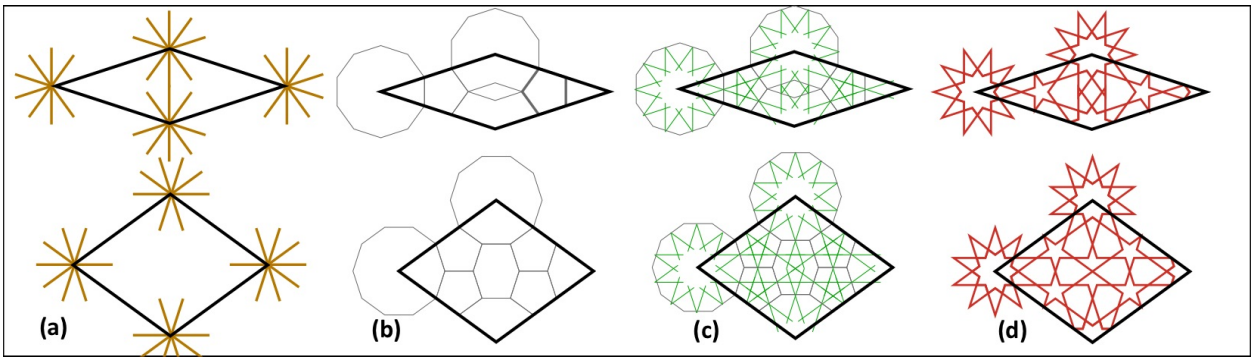

Figure 3: *Developing patterns for $IGP_R(10)$: (a) Place 10-fold symmetry lines at each vertex; (b) Create polygonal subgrid; (c) Place contact angles at polygon edge midpoints; (d) Complete patterns.*

Introduction to Polar Zonohedra

Polar zonohedra (PZ) are an especially beautiful, rotationally symmetric class of polyhedra all of whose faces are rhombi with the same edge lengths. It is easiest to picture a PZ as emanating from the origin with a P-fold axis of symmetry in the z direction. Each $PZ(P,\theta)$ is defined entirely by P, the number of equal length generating vectors (spaced at angles of $(360/P)°$ around the z axis), and θ, the "pitch angle" of those vectors relative to the xy plane. When θ is close to 0°, the PZ will have a very flat, pancake-like shape; when θ is close to 90°, it will have a very pointy, cigar-like shape; and in between it will have a shape reminiscent of a football (see Figure 4). Hart [4] enumerates many other interesting properties of this class of shapes, and derives the following formula for the bottommost rhombic face angle at the j^{th} level (with $j = 0$ being the "bottom" set of faces with vertices at the origin): Angle_j of $PZ(P,\theta) = ArcCos[Cos(360j/P)Cos^2(\theta) + Sin^2(\theta)]$.

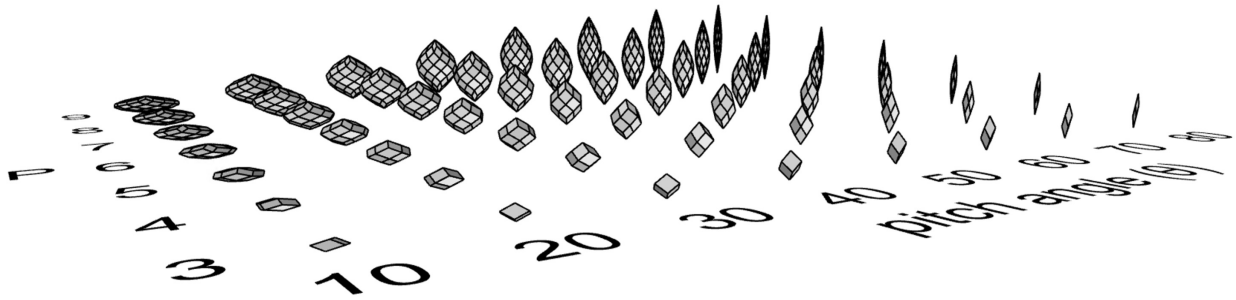

Figure 4: *Examples of polar zonohedra $PZ(P,\theta)$ for a variety of values of P and θ*

Comparing Rhombic Angles of IGP and PZ

When attempting to apply IGP arbitrarily to the faces of PZ, the results are usually aesthetically unsuccessful (see Figure 5). On the left, an 8-fold IGP has been applied to an arbitrary PZ (turned sideways here for greater detail), and distortions are very clear. At the tips, the green "shield" shapes are contorted into three very different aspect ratios; in the center, the square configurations are noticeably stretched; and some transitions between faces do not even preserve straight pattern lines across their boundaries (e.g. the left side of the blue figure just left of center). Conversely, on the right, a PZ discovered through the process described later in this paper accommodates the same IGP with minimal distortion and hence a much more satisfying effect.

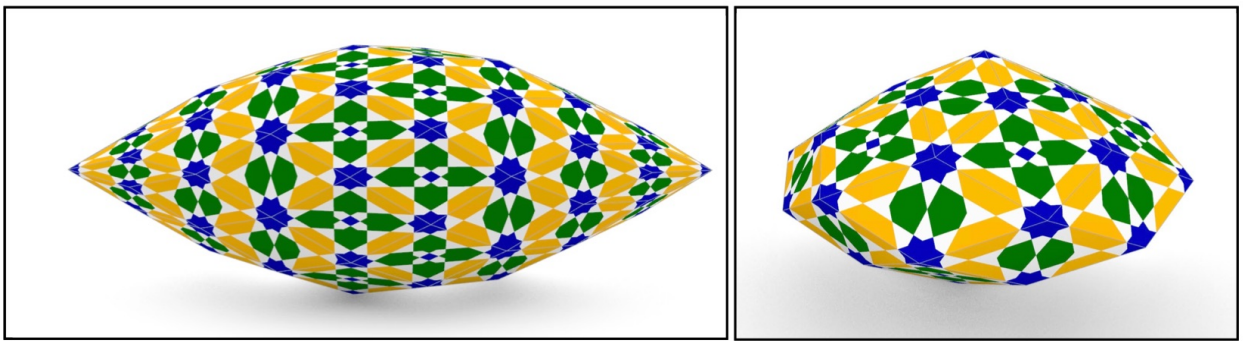

Figure 5: *An* 8*-fold IGP applied to an arbitrary PZ (left) vs. a carefully selected PZ (right).*

The reason aribtrary matches rarely work well is that there are only a few special cases where the set of face angles of a given $PZ(P,\theta)$ are exactly in the form $i(360/N)°$ required by the repeat units of $IGP(i,N)$. One is the degenerate case of $PZ(P,0)$ (for any P). In this case all of the faces are of exactly the form $i(360/N)°$; however, the PZ is completely flat and has no volume. Another is the unique case of $PZ(3, Arctan(1/\sqrt{2}))$, which produces a perfect cube, and so admits any IGP based on a square repeat unit. Cubes decorated with IGP are very beautiful, but don't capture the special essence of PZ.

So at first the task of decorating a typical, football-shaped PZ would seem nearly impossible. However, in relatively rare circumstances, it turns out that all of the face angles of a given PZ fall within a small number of degrees of some set of angles $i(360/N)°$. Once such a PZ is identified, it becomes possible to apply a set of patterns $IGP_R(N)$ to its faces, by using small linear scalings of the pattern to match the angles of pattern's repeat units to the angles of each PZ face. So, how does one go about identifying such PZ?

Graphing PZ Face Angles

We begin by getting a feel for how PZ face angles vary as θ moves from 0° to 90°. Figure 6 shows four examples for PZ with P = 5, 5, 7, and 14 (for the moment ignore the shaded areas and vertical lines and ovals; we'll discuss these shortly). One immediately gets a visual sense of how the face angles vary as the PZ moves from the "pancake" shape near $\theta = 0°$ to the "cigar shape" near $\theta = 90°$:

- Note that we only need to inspect the angles for the bottom half of the PZ (i.e., the first $\lfloor P/2 \rfloor$ angles), since the upper half is just a reflection of the bottom half.
- At $\theta = 0°$, the PZ is completely flat, and so the face angles are simply $360i/N°$ and hence evenly spaced along the vertical axis. This is the degenerate case mentioned earlier.
- At $\theta = 90°$, the PZ collapses to a vertical line, so all the face angles drop to 0°.
- In between, angles decrease along a series of curves (or a straight line for the top curve for even P) per the function listed above (Angle_j of $PZ(P,\theta) = ArcCos[Cos(360j/P)Cos^2(\theta) + Sin^2(\theta)]$).

Identifying Potential IGP-PZ Matches

Now that we have PZ face angles graphed, we can see how they relate to the angles for a given $IGP_R(N)$ (Figure 6, dashed blue horizontal lines), and look for values of the pitch angle θ where the two sets of curves intersect or pass close enough to each other that a match seems feasible (Figure 6, vertical lines and ovals). In the upper left we see a near match at $\theta = 44°$ (the maximum discrepancy was 5.04°, which just missed

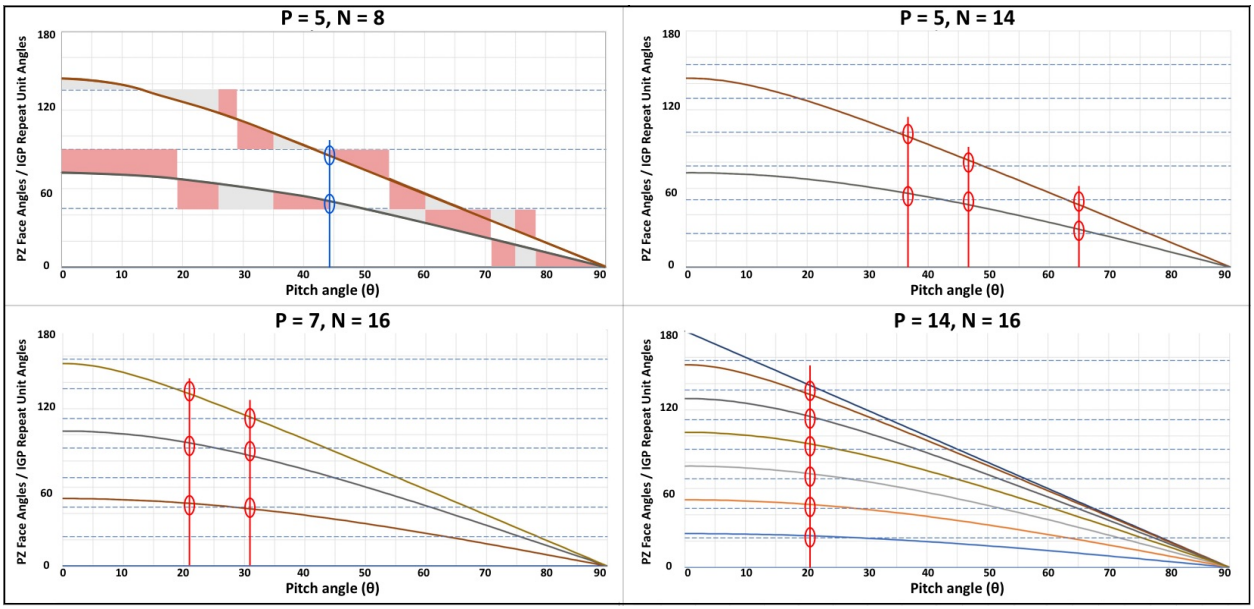

Figure 6: *Graphs of PZ face angles varying with θ for various values of P. Also shown are IGP rhombus angles $i(360/N)°$ (dashed horizontal lines) and close matches (red vertical lines and ovals). The upper left graph also shows a near match (blue vertical lines and ovals), areas of closest match (gray shaded areas), and "zones of influence" for maximum differences (red shaded areas).*

the threshold of 5°); in the upper right, 3 matches at $\theta = 37°, 47°$, and 65°, and so on. ***Note that not all IGP angles must be used*** in matching because (a) pairs of values that sum to 180° are already redundant, since they represent the same rhombus rotated by 90°, and (b) we need not use every rhombus in the given $IGP_R(N)$ set. ***Conversely, we DO need to find decent matches for all PZ face angles***, since each one represents a distinct face type of the given PZ. A few additional points of interest from Figure 6:

- The same P has different matching behavior w.r.t. different N (compare upper left and upper right).
- Larger P mean more angles to match, so there are on average fewer matches (compare last 3 graphs).
- Two PZ face angles can match the same IGP angle from above and below (lower right, top oval).
- The maximum difference shifts constantly as θ increases. In the upper left, gray shaded areas show where each curve is closest to an N line, and red areas show where the maximum difference lies.

An Exhaustive Search for Candidates

Rather than generate and inspect every pair of PZ curves and IGP lines, we can at this point create a function that returns for each triple (P, θ, N) the maximum deviation between the set of face angles for $PZ(P, \theta)$ and each angle's closest-matching IGP angle $(360/N°)$. We can tabulate these results and start looking for values below a given threshold (say, $\leq 5°$) where we might be able to scale the IGP without noticeable deformation. I implemented this in Excel with a few simple VBA functions, and Figure 7 shows an example of the data for $6 \leq N \leq 16$, $0° \leq \theta \leq 90°$, and $P \in \{3, 5, 7, 14\}$. Several interesting patterns emerge in Figure 7:

- The apparently random up and down patterns are due to shifting "zones of influence" – that is, which of the PZ angles is driving the maximum difference for any given range of θ. Examine the red highlighted zones of influence in Figure 6 (upper left) to see how they dictate the contour of the chart for $N = 8$ (Figure 7, upper right, second curve from the top, in orange).

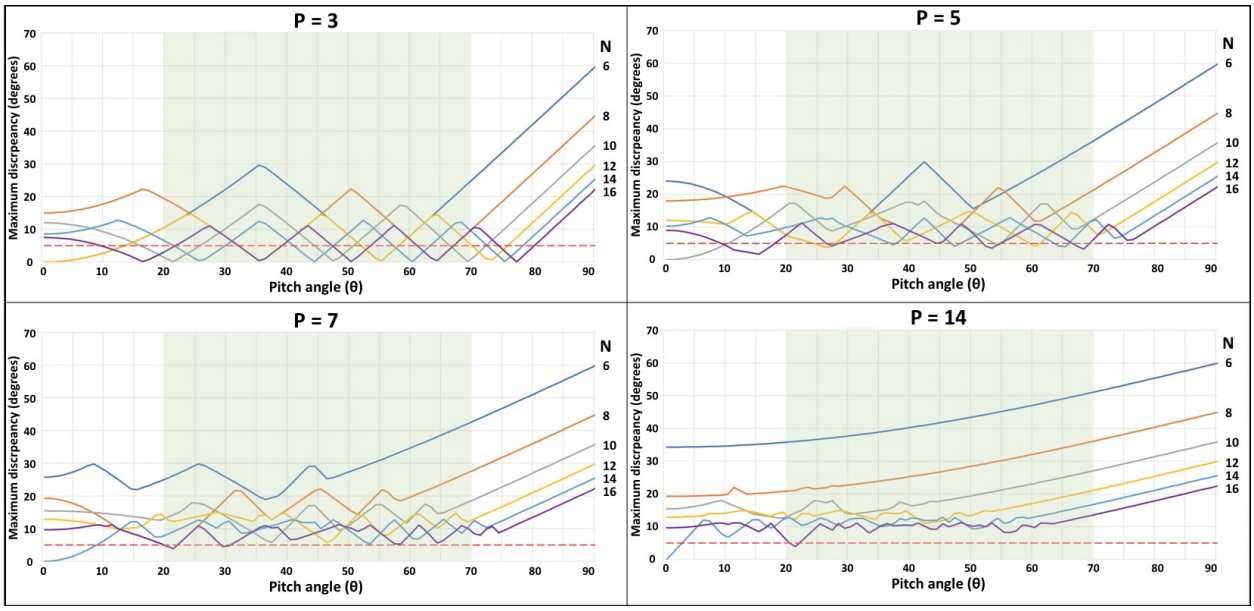

Figure 7: *Maximum discrepancies between PZ angles and IGP angles for* $N \in \{6, 8, 10, 12, 14, 16\}$ *and* $P \in \{3, 5, 7, 14\}$. *Shaded areas show ideal range of* θ*, and dashed lines show match threshold (*$5°$*).*

- For all P, the maximum is eventually driven by the smallest PZ angle and smallest IGP angle, and at that point it grows steadily to $360/N°$ (see the rightmost side of each series).
- Drawing a horizontal line at our threshold level (dashed red horizontal line near the bottom of each chart) makes it easy to locate places where various maxima drop below the threshold.
- The higher the value of P, the less likely an overall match becomes, since there are progressively more ($\lfloor P/2 \rfloor$) different angles to match. At $P = 3$ there is only one angle to match (these PZ are equilateral parallelepipeds with 6 congruent faces), so many exact matches exist where graphs graze the x axis; $P = 5$ and $P = 7$ show ever fewer matches; and by $P = 14$ there is but one match for a single N.

One final criterion is more aesthetic and practical than mathematical. Recall that extreme values of θ near $0°$ and $90°$ lead to very "flat" and "pointy" shapes, respectively. At an aesthetic level, I find these shapes less beautiful, and at a practical level, constructing IGP on extremely thin rhombi often does not lead to good results. Thus, I restricted my final tally to the range $20° \leq \theta \leq 70°$ (green shaded areas in Figure 7).

Using the final set of criteria ($6 \leq N \leq 16$, $3 \leq P \leq 15$, $20° \leq \theta \leq 70°$), and a maximum difference threshold of $5°$, a total of 43 final candidates were found (see supplemental spreadsheet). As expected, candidates decrease as P increases, since there are more simultaneous PZ face angles to match. The case of $P = 3$, which has only one face angle to match, can fit any pattern (see Figure 1). Also, larger values of N are easier to match because they provide a larger set of rhombic repeat shapes.

Making IGP conform to PZ Faces

Lastly, we need a way to adapt the patterns in $IGP_R(N)$ before we can apply them to the faces of the matched $PZ(P, \theta)$. This is a simple matter of scaling along one axis to make the pattern match the PZ face in question (see Figure 8).

We now have all the tools we need to decorate PZ with IGP, and fulfill the title of the paper! Several decorated PZ renderings are shown in Figures 1 and 9. Each $IGP_R(N)$ has been given its own color scheme

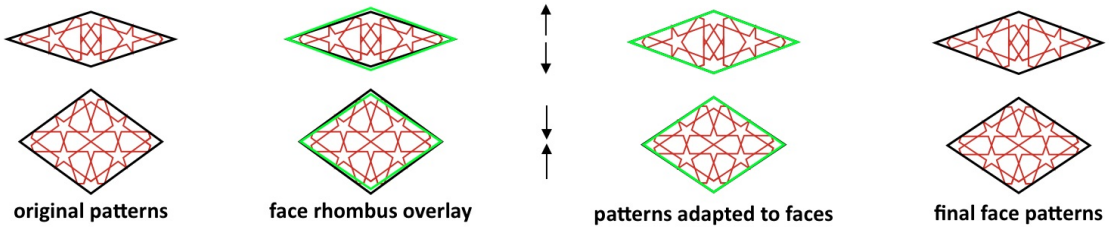

Figure 8: *Scaling $IGP_R(N)$ to fit faces from $PZ(5, 54°)$. Original rhombi have acute angles of 36° and 72°; acute face angles are ~ 40.42° (requiring widening) and ~ 67.98° (requiring narrowing).*

to help identify it across multiple PZ; the color schemes are mostly reminiscent of those used in traditional patterns, though the $IGP_R(16)$ pattern is less so. Figure 1 shows the flexibility inherent in PZ with $P = 3$. With only one shape of rhombic face, one can vary the pitch angle θ such that any desired acute face angle is achieved, and thus any IGP can be made to fit smoothly. Figure 9 demonstrates a cross section of possibilities covering many values of P and all values of N that were considered.

Conclusion and Future Directions

By systematically comparing sets of PZ face angles with sets of IGP rhombic repeat angles, we can identify IGP that can be linearly scaled to fit the faces of certain PZ. As Figure 9 shows, there is a large variety of possibilities. So far I have only produced 3D renderings, but I plan to create physical models in the near future. Given how good matches at a threshold of 5° appear, I plan to see if wider thresholds can still yield patterns without noticeable deformation. I also plan to develop $IGP_R(N)$ for larger N (e.g. 18, 20, 22 ...). This may be especially fruitful given that the number of viable PZ candidates increases as N increases.

References

[1] J. Bonner. *Islamic Geometric Patterns: Their Historical Development and Traditional Design Methodology*. Springer, 2017.

[2] J. Bonner and M. Pelletier. "A 7-Fold System for Creating Islamic Geometric Patterns Part 1: Historical Antecedents" *Bridges Conference Proceedings*, Towson, Maryland, USA, Jul. 25–29, 2012, pp. 141–148. https://archive.bridgesmathart.org/2012/bridges2012-141.html

[3] L. Eriksson. "Adapter Tiles Evolves the Girih Tile Set." *Bridges Conference Proceedings*, Online, Aug. 1–5, 2020 pp. 19–26. http://archive.bridgesmathart.org/2020/bridges2020-19.html

[4] G. Hart. "The Joy of Polar Zonohedra." *Bridges Conference Proceedings*, Online, Aug. 1–3, 2021, pp. 7–14. http://archive.bridgesmathart.org/2021/bridges2021-7.html

[5] C. S. Kaplan and D. H. Salesin. "Islamic star patterns in absolute geometry." *ACM Transactions on Graphics*, vol. 23, no. 2, Apr. 2004, pp 97-119. https://grail.cs.washington.edu/wp-content/uploads/2015/08/kaplan-2004-isp.pdf

[6] M. Pelletier and J. Bonner. "A 7-Fold System for Creating Islamic Geometric Patterns Part 2: Contemporary Expression." *Bridges Conference Proceedings*, Towson, Maryland, USA, Jul. 25–29, 2012, pp. 149–156. http://archive.bridgesmathart.org/2012/bridges2012-149.html

[7] P. Webster. "Fractal Islamic Geometric Patterns Based on Arrangements of n</Em>/2 Stars." *Bridges Conference Proceedings*, Enschede, the Netherlands, Jul. 27–31, 2013, pp. 87–94. http://archive.bridgesmathart.org/2013/bridges2013-87.html

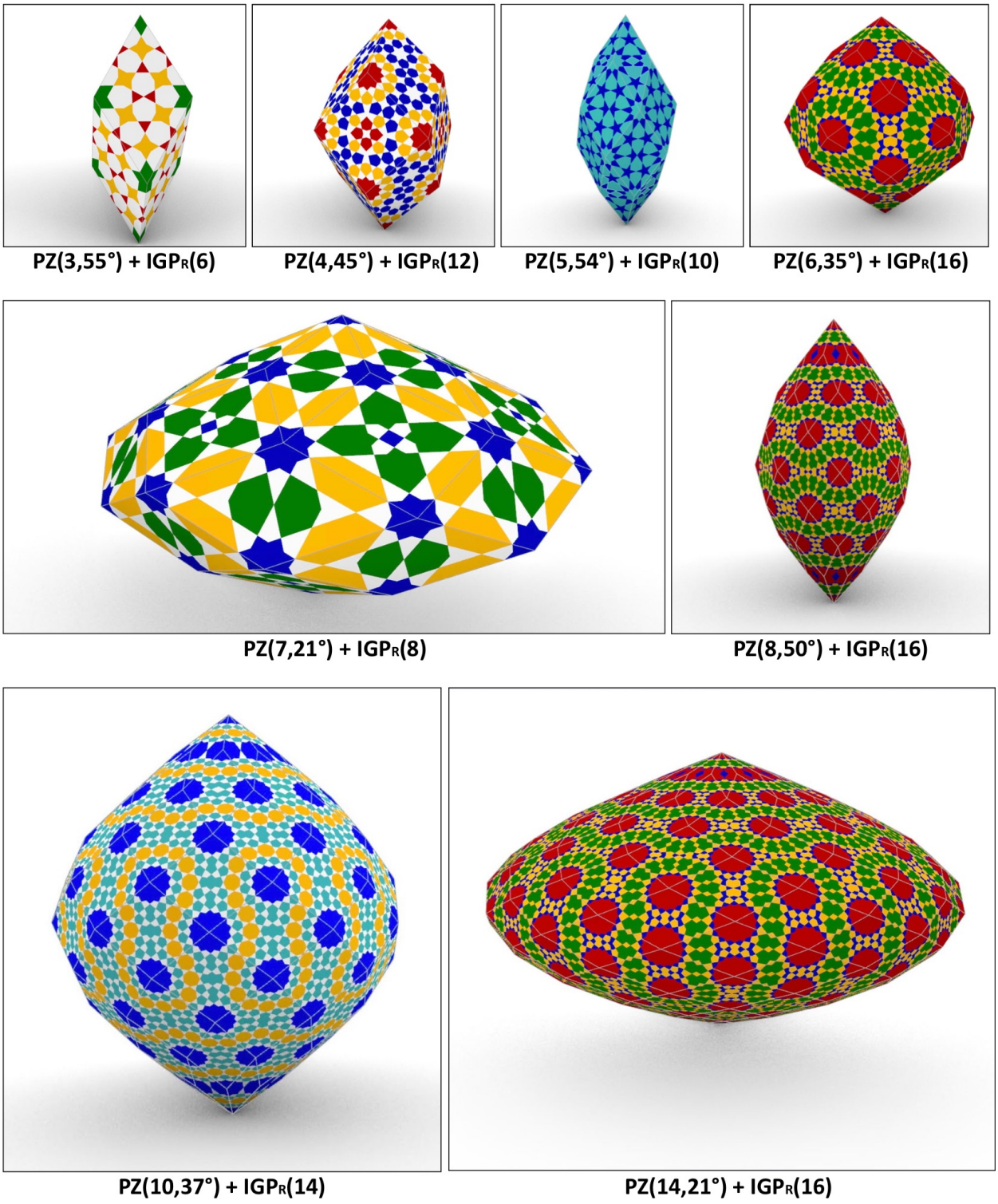

Figure 9: *Polar zonohedra selected from the 43 final candidates fulfilling all criteria listed previously. Each is labeled with its underlying shape $PZ(P,\theta)$ and its pattern $IGP_R(N)$.*